# POST BUCKLING ANALYSIS OF COMPOSITE MATERIAL PLATES IN THE PRESENCE OF THERMAL RESIDUAL STRESSES.

**Fernanda Mariana Nunes Ravetti**
ITA - Instituto Tecnológico de Aeronáutica. Praça Marechal Eduardo Gomes, 50 - Vila das Acácias. CEP 12228-900.
São José dos Campos – SP. Brasil.
fernanda.ravetti@embraer.com.br

**Sérgio Frascino Müller de Almeida**
ITA - Instituto Tecnológico de Aeronáutica. Praça Marechal Eduardo Gomes, 50 - Vila das Acácias. CEP 12228-900.
São José dos Campos – SP. Brasil.
frascino@mec.ita.br

***Abstract.*** *Composite material panels are cured or consolidated at temperatures that typically vary between 120 $^{o}$C and 400 $^{o}$C, when the laminates are completely stress free. When the panels temperature starts to decrease, since the material starts to get stiffer, the difference between the physical properties of the composite material in the fiber longitudinal and transversal direction, particularly the thermal expansion coefficient, causes the appearance of thermal residual stresses. In the case of a uniform (without stiffeners) symmetrically laminated panel without external constraints, the effect of the resultant stresses caused by residual stresses is null. However, if the panel is reinforced or not symmetrically laminated, the resultant stresses are not null and may have a significant influence on the panel mechanical behavior.*
*The previous works on thermal residual stresses study the critical load of linearized buckling problems (eigenvalue) for composite material structures/panels. This research studies the effect of thermal residual stresses on the post-buckling behavior of graphite-epoxy panels under compression, with stringers of different types and thickness.*
*The presence of thermal residual stresses may cause a large increase of stiffness and changes in the panels buckling modes, depending on the type and width of the stiffeners. For the studied plates, the gain in stiffness is proportionally higher for small loads and starts to decrease as the load increases. Also, plates with wider stiffeners have greater increase in stiffness.*

***Keywords****: composite material, post-buckling, thermal residual stresses, finite elements, non-linear analysis.*

## 1. Introduction

Co-cured composite material structures are heated to very high temperature levels during curing or consolidation process when they are completely stress free. When temperature starts to decrease, the thermal residual stresses appear due to the anisotropy of composite materials, such as the difference between thermal expansion coefficient of the material along the fibers longitudinal and transversal directions. The effects of these stresses are relevant particularly if the structure is asymmetric or non-uniform (with stiffeners). They may considerably change structures mechanical behavior, however they are not usually accounted for in the design of composite structures (*Adams e Bowles, 1975*).

Previous researches on the effects of thermal residual stresses in composite material structures (*Sai Ram e Sinha, 1992; Sun e Hsu, 1990*) use *thermal buckling* solutions which have limited application because the constraining structure is assumed not to be subjected to thermal expansion. This condition is seldom observed in actual aeronautical structures. Also, linearized buckling solution is always assumed (eigenvalue problem) which is usually too conservative for design applications.

The magnitude of thermal residual stresses depends on panel geometry, manufacturing, material physical properties, stiffeners type, problem boundary condition, difference between cure and operating temperature and etc. *Almeida* and *Hansen* (1997) brought in the idea of intentionally introduce manufacture induced thermal residual stresses in composite structures to improve their mechanical behavior. Plates with several different types and sizes of stiffeners were analyzed. Variations of material physical properties according to temperature were not considered, and the applied load and boundary condition represented the condition of a plate in a compression test. They concluded that the type and size of stiffeners have a great influence in distribution of thermal residual stresses, which affects the mechanical behavior of the plate increasing the buckling critical load. For a certain range of temperature, this gain gets higher with temperature increase. The plate-buckling mode can also be affected. Similarly, they also investigated the effect of these stresses on the natural frequencies of the plate (*Almeida* and *Hansen*, 1999). The boundary conditions and general considerations were the same of previous research and they concluded that the thermal stresses could also significantly modify plate vibration mode and natural frequencies. Finally, *Almeida* and *Hansen* (2002) studied the interaction between structural damages and thermal residual stresses on the buckling critical loads of composite plates. They considered local impact damages and delamination. It was found that in the presence of damage, for the studied cases, the performance of the plates with thermal stresses was in general superior to that of the plates without thermal stresses.

The optimization of composite plates in the presence of thermal stresses was studied by *Andrade*, *Hernandes* and *Almeida* (2003). They considered the optimization of linearized buckling load using a novel optimization procedure.

They concluded again that thermal residual stresses have great influence in composite panels buckling and that the eigenvalue vary almost linearly with temperature variation within a certain range of temperature.

The previous researches study the critical load of linearized buckling problems (eigenvalue) for structures/panels of composite material. This research studies the effect of thermal residual stresses on the post-buckling behavior of composite plates. The performed post-buckling analyses use the non-linear static solution of the finite element solver *MSC.Nastran*®. It is found that the presence of thermal residual stresses may change the panels buckling modes, and provide a significant increase of stiffness, depending on the choice of the stiffeners.

## 2. Thermal stresses in composite laminates

Polymeric materials are the mostly used type of composite material in aeronautical primary structures, primarily because of their high stiffness/weight ratio. The composite materials most important anisotropic property in determining the thermal residual stresses is the thermal expansion coefficient ($\alpha$). $\alpha$ is very small along the fibers longitudinal direction (where fibers behavior is dominant) whereas is relatively high along the fibers transversal direction (where matrix behavior is dominant). This effect is very important in multidirectional and reinforced laminates, where there are action/reaction forces between plies, particularly in the presence of boundary conditions, non-uniform laminates or stiffeners.

If a laminate is subject to mechanical forces *{N}* and moments *{M}* and thermal variation $\Delta T$, its deformation is given by summation of both contributions. For an arbitrary *K* lamina (*Daniel* and *Ishai*, 1994):

$$\{\varepsilon\}_{x,y}^{K} = [S]_{x,y}^{K} . \{\sigma\}_{x,y}^{K} + \{e\}_{x,y}^{K} \tag{1}$$

where $\{\varepsilon\}_{x,y}^{K}$ is total deformation; $[S]_{x,y}^{K}$ is the material flexibility matrix; $\{\sigma\}_{x,y}^{K}$ is the stress tensor; $[S]_{x,y}^{K} . \{\sigma\}_{x,y}^{K}$ is the mechanical deformation; $\{e\}_{x,y}^{K} = \Delta T . \{\alpha\}_{x,y}^{K}$ is thermal deformation; $\Delta T$ is temperature variation (difference between the operation and cure temperatures); and $\{\alpha\}_{x,y}^{K}$ is the thermal expansion tensor for the laminae.

Considering that the mechanical deformation is linear through the thickness (Kirchhoff's hypotheses):

$$\{\sigma\}_{x,y}^{K} = [Q]_{x,y}^{K} \left( \{\varepsilon^{0}\}_{x,y}^{K} + \{\kappa\}_{x,y}^{K} z - \{e\}_{x,y}^{K} \right) \tag{2}$$

From the above, the mechanical resultant forces and moments may be computed from the strain and curvatures of the mid-plane and the thermal resultant forces and moments (*Daniel* and *Ishai*, 1994).

## 3. Numerical Methods for non-linear analysis

There are three sources of non-linearities in structural analyses: (1) geometric, (2) material behavior, and (3) changes in boundary conditions. The panels in this paper present only geometric non-linearities. This type of non-linearity is characterized by large displacements, when changes in the structure geometry cause changes in structure mechanical behavior (load-displacement relation). The non-linear equation for finite elements is (*Bathe*, 1996):

$$\sum_{e=1}^{N_e} \left\{ [T_n]^T \left\{ F_e^{\text{int}} \right\} - \left\{ F_e^{a} \right\} \right\} = \{0\} \tag{3}$$

where $N_e$ is the total number of elements; $[T_n]^T$ is the transformation matrix of element coordinate system to global coordinate system; $\{F_e^{int}\}$ is the element internal forces vector – in element coordinate system; and $\{F_e^{a}\}$ is the vector of loads applied on element - in global coordinate system. The non-linear equation for finite elements can be re-written as

$$\sum_{e=1}^{N_e} \left\{ [T_n]^T \left\{ \int_{V_e} [B_V]^T \{\sigma\} dV_e \right\} - \left\{ F_e^{a} \right\} \right\} = \{0\} \tag{4}$$

where $[B]$ is the element displacement-strain matrix; $\{\sigma\}$ is the element stress tensor; and $V_e$ is the element volume.

The non-linear stiffness matrix $[K_e^{nl}]$ is given by derivation of the non-linear static equation of finite elements:

$$\left[K_e^{nl}\right] = \frac{\partial}{\partial\left[u\right]}\left\{ \left[T_n\right]^T \left\{ \int_{V_e} \left[B_V\right]^T \{\sigma\} dV_e \right\} - \left\{F_e^a\right\} \right\} \tag{5}$$

then,

$$\left[K_e^{nl}\right] = \left[K_e^{inc}\right] + \left[K_e^{\sigma}\right] + \left[K_e^{u}\right] - \left[K_e^{a}\right] \tag{6}$$

where $[K_e^u]$ is the displacement-rotation initial matrix (that includes stiffness changes due to geometric changes); $[K_e^\sigma]$ is the stresses initial matrix (that includes stiffness changes due to the presence of initial stresses); $[K_e^{inc}]$ is the main tangential matrix; and $[K_e^a]$ is the loadings initial matrix (that includes stiffness changes due to load orientation changes).

In this study, the panel looses stability during the analysis, as it buckles, and the point where the structure looses stability is the bifurcation point. Crisfield arc-length method (*Bathe*, 1996) is typically used to handle this kind of problem with *MSC.Nastran*®.

## 4. Simulations

The considered panels have dimension of 360mm × 360mm and have stiffeners of different types, width and laminate. The stiffeners width is *b*, which can assume values 18mm, 36mm and 54mm. The geometry and the laminates used in the plates are defined in Fig. 1. All laminas are of graphite-epoxy, which properties are listed in Tab. 1.

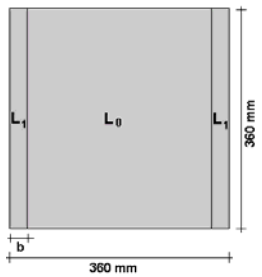

Panel A

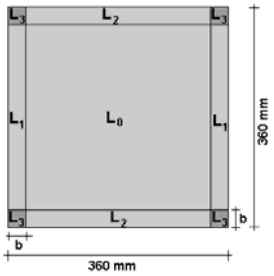

Panel B

Types of laminate

| | |
|---|---|
| **$L_0$** | $[90/0]_s$ |
| **$L_1$** | $[0_4/90/0]_s$ |
| **$L_2$** | $[90_4/90/0]_s$ |
| **$L_3$** | $[(90/0)_3]_s$ |

Figure 1. Plate geometry and laminate description

Table 1. Graphite-Epoxy T300/5208 properties (*Almeida e Hansen*, 1997)

| **Property** | **Value** |
|---|---|
| Elasticity Module in Longitudinal Direction, $E_1$ | 154500 MPa |
| Elasticity Module in Transversal Direction, $E_2$ | 11130 MPa |
| Poisson Coefficient, $\nu$ | 0.304 |
| In-plane Shear Module, $G_{12}$ | 6980 MPa |
| Transversal Shear Module, $G_{13}$ | 6980 MPa |
| Transversal Shear Module, $G_{23}$ | 3360 MPa |
| Thermal Expansion Coefficient in Longitudinal Direction, $\alpha_1$ | $-0.17 \times 10^{-6}/^oC$ |
| Thermal Expansion Coefficient in Transversal Direction, $\alpha_2$ | $23.1 \times 10^{-6}/^oC$ |
| Ply Thickness, $t$ | 0.15 mm |

Variations in material mechanical properties are not considered in this study. It is considered that panels have a temperature decrease of -150°C, due to an operation temperature of 177°C and a room temperature of 27°C. For comparison purposes, panel with no temperature variation are also analyzed.

### 4.1 - Eigenvalue Problem

The mechanical load is a compression load applied on upper and lower panel boundary. In the cases that do not consider temperature variation, the eigenvalue solution is directly calculated. In the buckling analysis that includes thermal loading, several iterations are necessary because in *MSC.Nastran*® the eigenvalue multiplies both the mechanical load and the thermal load, which must be -150°C at the end of the solution. Therefore, the pre-buckling load has to be iterated until a unit eigenvalue results for $\Delta T$ = -150 °C which is the temperature variation for all considered

cases. The applied boundary conditions represent the conditions of a panel in a compression test (using *MSC.Nastran*® notation): the upper and lower edges are restricted in TX, TZ, RX, RY and RZ; the nodes of the XZ symmetry plane are restricted in TY; and the edges are restricted in TZ and RX.

### 4.2 - Post-Buckling Problem

In the first subcase, the temperature variation of -150°C is applied to the plate. It has just one load increment and works as a thermo-elastic linear analysis (the analysis that does not consider temperature variation does not include this subcase). For the thermal load problem, the applied restraints must represent a condition where the panel is free. The imposed boundary conditions simply preclude rigid body motions. In the second subcase, the load is a transversal force of very low magnitude (1N) applied to the plate on its the central node. The function of this force is just introducing some asymmetry in the plate.

The third subcase is a compression force applied on the lower and upper border of the plate. Its magnitude varies depending on the plate that is being analyzed. A displacement load would be more appropriate to model this compression, but in *MSC.Nastran*®, the enforced displacement application would change the boundary conditions and cancel effects of temperature variation (first load case).

For both mechanical loads, the boundary conditions represent the condition of a plate in a typical compression test: the upper and lower panel borders are restricted in TX, TZ, RX, RY and RZ; the nodes of the XZ symmetry plane are restricted in TY; and the lateral borders are restricted in TZ and RX. (again, *MSC.Nastran*® notation is used).

### 4.3. Results

Figure 2 shows the finite element model of the plates. Linear buckling analyses are performed to determine the critical load of each plate with and without thermal residual stresses; the results are presented in Tab. 2. Since linear buckling analyses are conservative in comparison to real problems, the results of analyses without temperature variation are used to estimate the load to be applied in the post-buckling solution. The non-linear model maximum load is assumed to be approximately 10 times the critical load of the analysis without temperature.

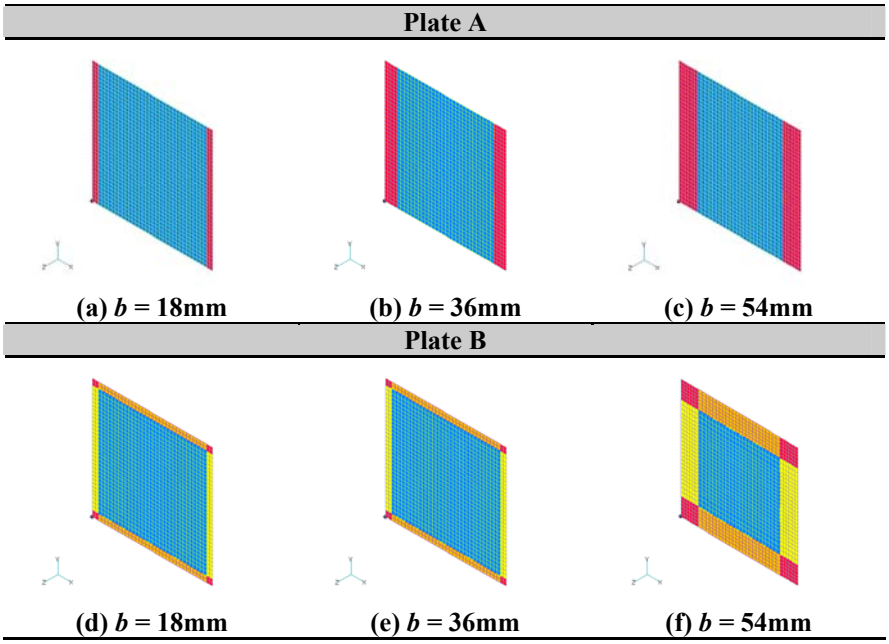


Figure 2. Finite element model of all plates.

Table 2. Critical Load for plates without thermal load.

| Plate A | | | Plate B | | |
|---|---|---|---|---|---|
| b (mm) | 1st Critical Load (N) | | b (mm) | 1st Critical Load (N) | |
| | ΔT=0°C | ΔT=-150°C | | ΔT=0°C | ΔT=-150°C |
| 18 | 197.5 | 770 | 18 | 200.1 | 943 |
| 36 | 274.7 | 946 | 36 | 288.0 | 1404 |
| 54 | 361.4 | 1188 | 54 | 417.6 | 2092 |

The method used for non-linear analysis is the Arc-Length method of *Crisfield*, available for solution 106 of *MSC.Nastran*®. The following table shows maximum displacement of the plates after non-linear analysis, considering stiffeners of type A and B, with width of 18mm, 36mm and 54mm, for both analyses with and without temperature variation.

Thermal residual stresses decreased considerably the magnitude of plates displacements. For plate A with 18mm stiffeners and for plate B with 18mm and 54mm stiffeners, the residual stresses also causes changes on plate buckling mode. Table 3 compares the maximum displacement of the plates with and without thermal loading. The smaller displacements of plates with thermal residual stresses confirm the stiffening effect of these stresses.

Due to the difference caused by residual stresses in buckling modes, the "Load × Displacement" plots are plotted with the displacement in Y direction of a central node of the upper border of the plate in Fig.3. The results of the linear buckling analysis are also represented in the graphics presented in Fig. 3 for comparison purposes.

A convergence test is performed for the first analyzed plate (type A, b=18mm) for model validation. The original model has 1296 elements, and the refined one has 11664. The difference of the results is 2.5% for the model without temperature case, and 3.5% for the model with temperature case, so it is considered that plate A model is valid for the analysis. The same refinement level is used for the other plates. For all plates, the convergence during analysis was much more difficult in the case including temperature variation; this can be observed from the high number of iterations in the graphic.

Tables 4 and 5 compare the displacements given by the plots for steps of 500N each. For lower loads, plate A with stiffener of 18mm has greater gain in stiffness compared to the other plates type A. For higher loads, plate A with stiffener of 54mm has greater gain compared to the other plates type A. The gain in stiffness depends on the considered load: the grater the load, the smaller is gain in stiffness of plates with thermal residual stresses compared to plates without residual stresses, in percentage. If the three plates A are compared, the one with larger stiffeners has in general a superior gain in stiffness, in the presence of thermal residual stresses.

Figure 4 presents cross section of the deformed plates in the YZ symmetry plane, for cases with and without temperature variation, for 50% and 100% of the total applied load. The changes in buckling modes and the non-linearity of the analysis are apparent.

Table 3. Comparison between the maximum displacement of the plates with and without thermal loading

| b (mm) | Plate A Total Displacement (mm) | | Difference | Plate B Total Displacement (mm) | | Difference |
|---|---|---|---|---|---|---|
| | ΔT = 0°C | ΔT =-15 0°C | (%) | ΔT = 0°C | ΔT =-15 0°C | (%) |
| **18** | 4.395 | 2.763 | -37% | 2.468 | 2.463 | -0% |
| **36** | 3.939 | 3.154 | -20% | 2.661 | 1.976 | -26% |
| **54** | 3.822 | 3.034 | -21% | 3.742 | 1.753 | -53% |

Table 4. Displacement difference between cases with and without temperature for plate A.

| | Applied Load (N) | Displacement (mm) | | | | | | | | |
|---|---|---|---|---|---|---|---|---|---|---|
| | | b = 18mm | | | b = 36mm | | | b = 54mm | | |
| | | ΔT | | % | ΔT | | % | ΔT | | % |
| | | 0°C | -150°C | | 0°C | -150°C | | 0°C | 150°C | |
| Plate A | **500** | 0.0225 | 0.0025 | -88.9 | 0.0150 | 0.0025 | -83.3 | 0.0100 | 0.0025 | -75.0 |
| | **1000** | 0.0850 | 0.0225 | -73.5 | 0.0650 | 0.0100 | -84.6 | 0.0475 | 0.0075 | -84.2 |
| | **1500** | 0.1750 | 0.1025 | -41.4 | 0.1450 | 0.0575 | -60.3 | 0.1000 | 0.0275 | -72.5 |
| | **2000** | 0.2875 | 0.2250 | -21.7 | 0.2525 | 0.1450 | -42.6 | 0.1700 | 0.0800 | -52.9 |
| | **2500** | | | | 0.3725 | 0.2575 | -30.9 | 0.2625 | 0.1575 | -40.0 |
| | **3000** | | | | | | | 0.3525 | 0.2525 | -28.4 |
| | **3500** | | | | | | | 0.4675 | 0.3600 | -23.0 |

| b | "Applied Load (N) x Displacement Y (mm)" | |
|---|---|---|
| | Plate A | Plate B |
| 18 | 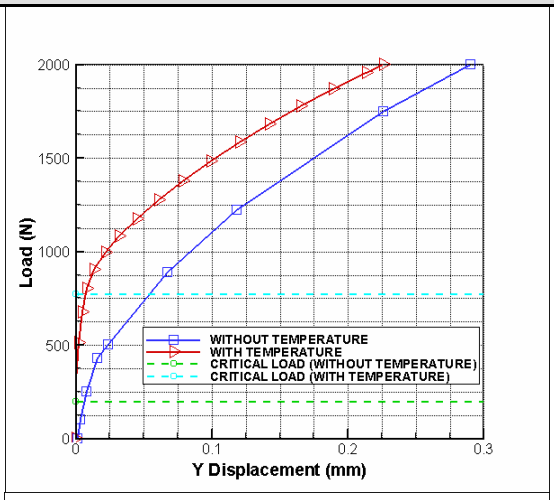 | 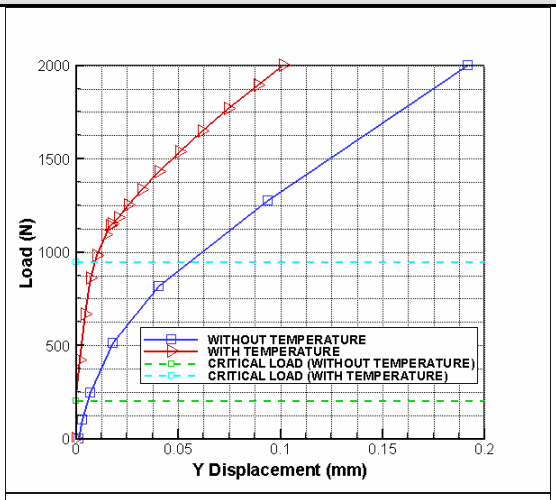 |
| 36 | 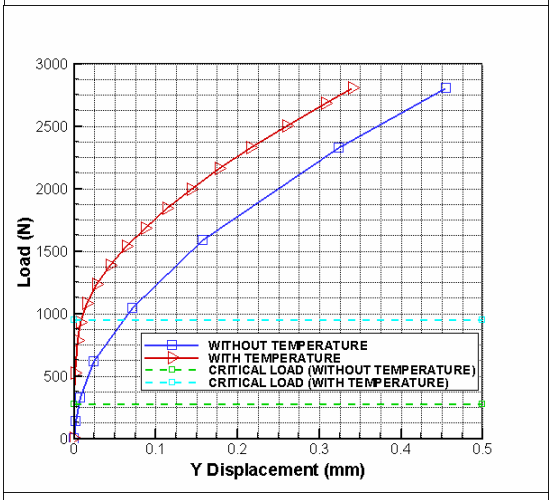 | 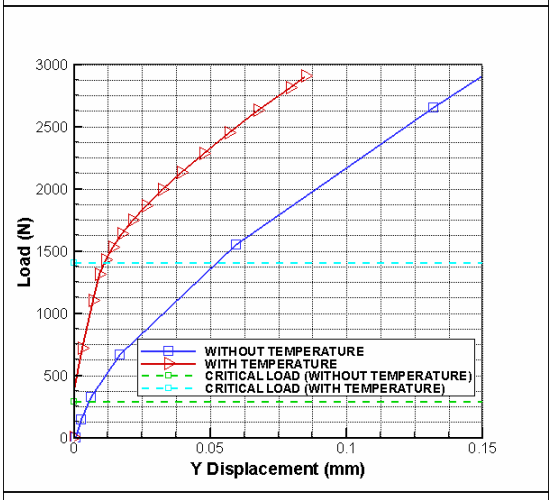 |
| 54 | 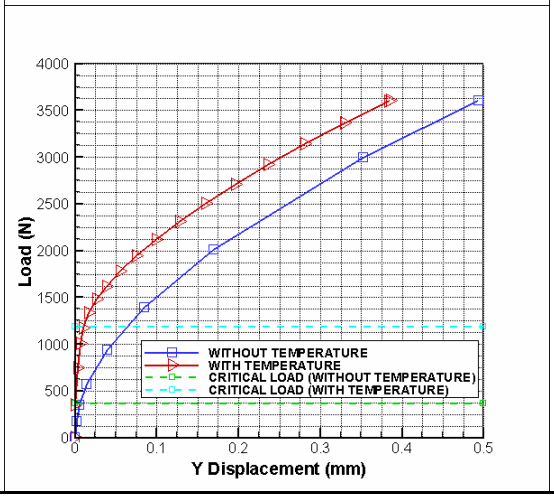 | 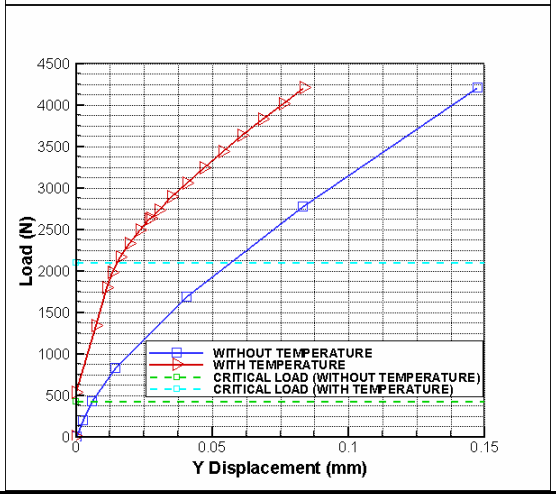 |



Figure 3. Load × Displacement plots

Table 5. Displacement difference between cases with and without temperature for plate B.

| | Applied Load (N) | b = 18mm | | | b = 36mm | | | b = 54mm | | |
|---|---|---|---|---|---|---|---|---|---|---|
| | | ΔT | | % | ΔT | | % | ΔT | | % |
| | | 0°C | 150°C | | 0°C | 150°C | | 0°C | 150°C | |
| Plate B | 500 | 0.0163 | 0.0025 | -84.6 | 0.0125 | 0.0013 | -90.0 | 0.0750 | 0.0000 | -100.0 |
| | 1000 | 0.0625 | 0.0113 | -82.0 | 0.0325 | 0.0050 | -84.6 | 0.0188 | 0.0038 | -80.0 |
| | 1500 | 0.1250 | 0.0475 | -62.0 | 0.0563 | 0.0138 | -75.6 | 0.0350 | 0.0088 | -75.0 |
| | 2000 | 0.1913 | 0.1013 | -47.1 | 0.0888 | 0.0325 | -63.4 | 0.0525 | 0.0138 | -73.8 |
| | 2500 | | | | 0.1219 | 0.0594 | -51.3 | 0.0725 | 0.0238 | -67.2 |
| | 3000 | | | | | | | 0.0938 | 0.0388 | -58.7 |
| | 3500 | | | | | | | 0.1163 | 0.0563 | -51.6 |
| | 4000 | | | | | | | 0.1388 | 0.0750 | -45.9 |

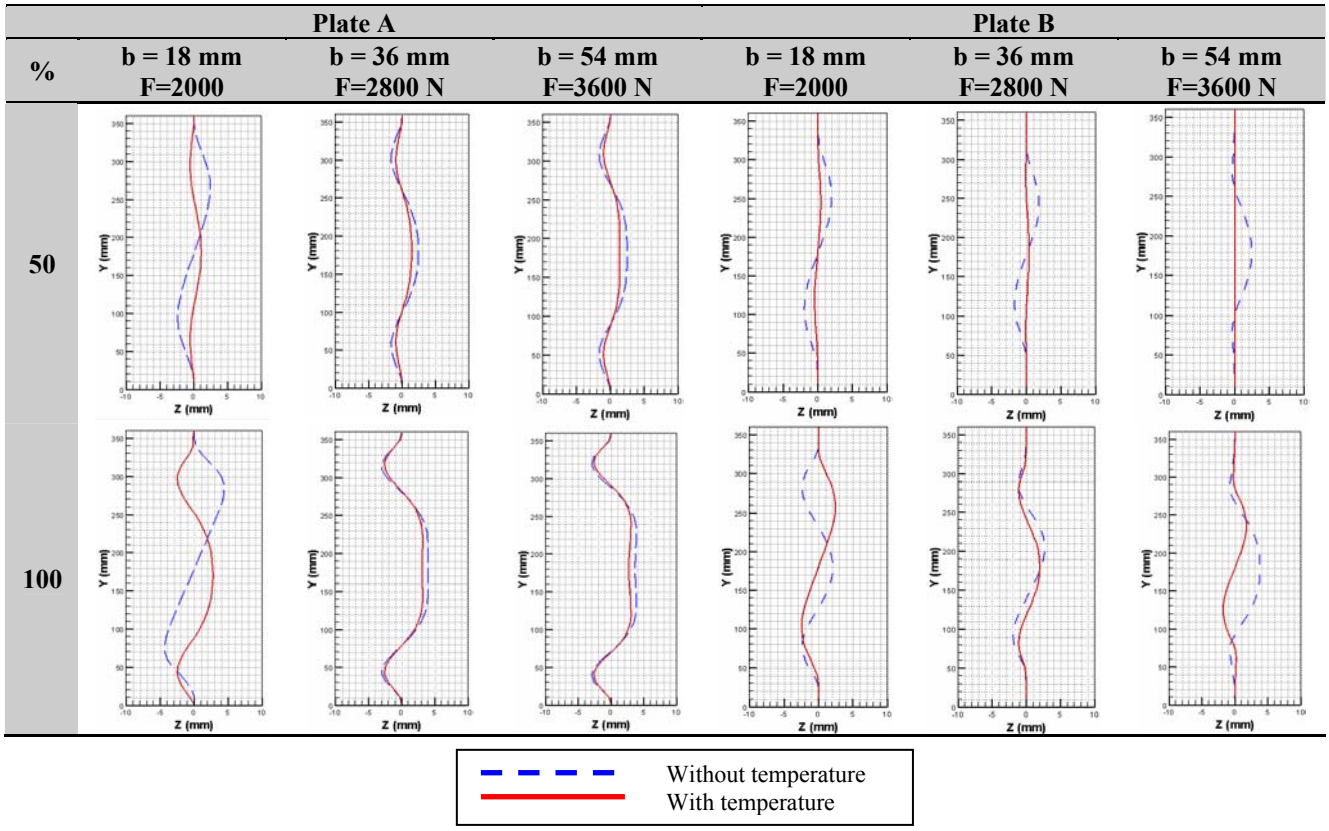


Figure 4. Transverse displacements for plates type A and B

## 5. Conclusion

For linear buckling analysis, the plates with the largest stiffeners have the critical load higher than the others, in both cases with and without thermal residual stresses, although for the last case the critical loads are much grater. These stresses in some cases also change the buckling mode of the plate. The "Load × Displacement" plots show that there is a significant reduction of displacements magnitude in plates with thermal residual stresses, implicating that the residual stresses increases the stiffness to plates under compression. This gain depends on the applied load: the greater is the load, the smaller is the gain. For plates type A and lower loads, the plates with narrower stiffeners have better gain than the others, and as the load increases, the gain is larger for the wider stiffeners. For plates type B, in general the plates with wider stiffeners have a greater gain. The convergence is more difficult for analysis considering thermal effects. The non-linearity of the problem is clear from the cross section of the deformed plates.

The thermal residual stresses can be intentionally introduced in the component design to enhance the structural behavior. Comparing plates A and B, the one that has the better stiffness gain is plate B with stiffeners of 54mm width.

For an actual aeronautical structure, the cost/benefit relation must be analyzed to verify if the thermal effects are advantageous.

## 6. References


Adams, D. S., Bowles, D. E., and Herakovich, C. T., 1988, "Thermally induced transverse cracking in graphite-epoxy cross-ply laminates", in "Environmental effects on composite materials", Vol. 3, ed. Springer, G. S., Technomic Publ. Co. Inc., Lancaster, Pennsylvania, pp. 247-274.

Almeida, S. F. M., Hansen, J. S., 1997, "Enhanced Elastic Buckling Loads of Composite Plates With Tailored Thermal Residual Stresses", ASME Journal of Applied Mechanics, Vol. 64, pp.772-780.

Almeida, S. F. M., Hansen, J. S., 1999, "Natural Frequencies of composite plates with tailored thermal residual-stresses", International Journal of Solids and Structures, pp.3517-3539.

Almeida, S. F. M., Hansen, J. S., 2002, "Buckling of Composite Plates with Local Damage and Thermal Residual Stresses", AIAA Journal, Vol. 40, pp.340-345.

Andrade, L. H., Almeida, S. F. M., Hernandes, J. A., 2003, "Optimal Buckling Design of a Composite Plate Operating in a Given Temperature Range", Proceedings of COBEM 2003, COBEM, pp.1318 – 1327.

Bathe, Klaus-Jürgen, 1996, "Finite Element Procedures", Prentice Hall, Englewood Cliffs, New Jersey, 1037p.

Daniel, I. M., Ishai, O., 1994, "Engineering Mechanics of Composite Materials", Oxford University Press, Inc., pp.142-225.

Sai Ram, K. S., and Sinha, P. K., 1992, "Hygrothermal effects on the free vibration of laminated composite plates", Journal of Sound and Vibration, V. 158, No. 1, pp. 133-148.

Sun, L. X., and Hsu, T. R., 1990, "Thermal buckling of laminated composite plates with transverse shear deformation", International Journal of Computers & Structures, Vol. 36, pp. 893-899.


## 5. Responsibility notice

The authors are the only responsible for the printed material included in this paper.